

## Research Article

# Assignment of O–O and Mo=O Stretching Frequencies of Molybdenum/Tungsten Complexes Revisited

**Choon Wee Kee**

*Division of Chemistry and Biological Chemistry, School of Physical and Mathematical Sciences, Nanyang Technological University, 21 Nanyang Link, Singapore 637371*

Correspondence should be addressed to Choon Wee Kee; [cwkee@ntu.edu.sg](mailto:cwkee@ntu.edu.sg)

Received 22 December 2014; Revised 25 March 2015; Accepted 2 April 2015

Academic Editor: Arturo Espinosa Ferao

Copyright © 2015 Choon Wee Kee. This is an open access article distributed under the Creative Commons Attribution License, which permits unrestricted use, distribution, and reproduction in any medium, provided the original work is properly cited.

The assignment of peroxo stretching frequencies for Molybdenum and Tungsten complexes is studied by DFT and MP2 calculations. We found that M06 functional is unsuitable for assignment of Mo=O and O–O stretches in  $\text{CpMo}(\eta^2\text{-O}_2)\text{OCH}_3$  and we found that MP2 and even the def2-TZVP do not give accurate order of asymmetric and symmetric Mo=O stretching. We recommend the M06L, which is a good compromise between speed and accuracy, for works involving these complexes. For a series of ten Molybdenum and Tungsten complexes studied we found that, for Mo/W=O stretching frequencies at M06L/def2-TZVP, after scaling, a small RMSD of  $15\text{ cm}^{-1}$  could be obtained. However peroxo stretching frequencies RMSD remains high at  $40\text{ cm}^{-1}$  after scaling. This could potentially point out the need for reassignment of experimental peroxo frequencies in some of the works cited in this report.

## 1. Introduction

IR spectroscopy is an important characterization technique in chemistry and it has been extensively employed in various subdisciplines of chemistry such as organic, inorganic, and organometallic chemistry. In this work, we are interested in the assignment of vibrational modes (Mo/W=O and O–O stretching modes) in Molybdenum and Tungsten complexes which are efficient catalysts in epoxidation and oxidation [1–4].

We had been working on the use of Molybdenum based catalyst in both epoxidation [5] and oxidation of phenol [6]. Computational studies on the epoxidation of olefins catalyzed by Molybdenum complexes have been reported by the groups of Costa et al. [7], Drees et al. [8], and Comas-Vives et al. [9]. Generally, the B3LYP functional is employed in these studies, and while B3LYP is one of the main driven forces for the early popularity of employing DFT in chemistry [10], its shortcoming when applied to kinetics and interactions which involves dispersion is well documented in the literature [11–16]. Therefore, we decided to revisit these reactions with the Minnesota density functionals which have broad accuracy for application

in thermochemistry, kinetics, and noncovalent interactions [17].

During the course of our study, we found that not all Minnesota density functionals are suitable for the assignment of Mo=O stretching and O–O stretching in Molybdenum and Tungsten complexes which contain these groups. We also found that some literature assignments of asymmetric and symmetric Mo=O stretching frequencies to observed bands in the IR spectrum do not agree with those calculated with modern DFT functionals. Relevant results would be presented in the rest of this work.

## 2. Material and Methods

All calculations were performed with Gaussian 09 A.02 or C.01 [18] on NUSHPC (National University of Singapore High Performance Computing).

Def2-SVP, def2-SVPD, def2-TZVP, def2-TZVPD, and def2-QZVPD basis sets [19] were obtained from basis set exchange [20, 21]. The DFT functionals used were implemented in Gaussian 09 C.01 [18].

The DFT functionals employed in this study are Minnesota series [11] (M06L [22], M06-2X, and M06), PBE0 [23],

B3LYP [24], CAM-B3LYP [25], B3PW91 [26], and wB97xD [27]. More detailed references to theoretical methods could be found in the DFT and MP2 section of Gaussian 09 website.

Frequency calculations were performed at the default atmosphere and temperature as implemented in Gaussian. Default convergence criteria and integration grid were used, unless otherwise stated. For tighter convergence criteria and larger integration grid, the keywords “opt=tight” and “int=ultrafine” were used in Gaussian 09.

For the study of solvent effect, two approaches were adopted. For explicit solvation, three solvent molecules (acetonitrile or water) were added. For implicit solvation model, the PCM model implemented in Gaussian 09 was used. Geometries optimization and frequencies calculations for explicit solvation are the same as in the gas phase calculations. For implicit solvation model, optimization and frequencies calculations are performed with PCM via the keywords “scrf=(solvent=acetonitrile).” Note that, for water, tighter convergence criteria and larger integration grid were specified via “opt=tight” and “int=ultrafine,” in addition to “scrf=(solvent=water).”

The isotopes used for frequency calculations are the default in Gaussian 09 unless otherwise stated.

Geometries for **1**-CF<sub>3</sub> (see Table 5), **1**-Cl (see Table 6), **8** (see Table 9 and Figure 6), **9** (see Table 9 and Figure 6), and **10** (see Table 9 and Figure 6) were obtained from XRD.

Anharmonic correction is generally neglected in this study. We attempted to fit the calculated harmonic frequencies to the fundamental frequencies observed experimentally.

3D images of optimized geometries are created with CYLview v1.0.562 beta [28] which generates the script for POYRAY. Images showing normal modes are generated with GaussView 5.0.9.

### 3. Results and Discussion

**3.1. Vibrational Modes of CpMo( $\eta^2$ -O<sub>2</sub>)OCH<sub>3</sub>.** Synthesis and characterization of CpMo( $\eta^2$ -O<sub>2</sub>)OCH<sub>3</sub> **1** were reported by Legzdins et al. [29] and Al-Ajlouni et al. [30]. Relevant IR bands and their assignment by Al-Ajlouni et al. are tabulated in Table 2; Legzdins and coworkers assignment was similar.

During the course of our study, we explored the use of M06 functional as recommended by Zhao and Truhlar for transition metal [11]. We found that, with the M06 functional, IR frequencies of Mo=O stretch and O–O stretch for **1** obtained do not agree with assignments made in the literature [30, 31]. More specifically, we found that the O–O stretching frequency is higher than that of Mo=O in terms of wavenumber, which contradicts the generally accepted assignment that M=O stretch is higher in wavenumber than O–O stretch for Molybdenum complexes of the general formula Cp’Mo( $\eta^2$ -O<sub>2</sub>)OR.

In our calculations, the geometry optimization and subsequent frequency analysis were performed with M06 functional and the family of basis sets defined by Weigend and Ahlrichs [19]. The optimized geometries of **1** at def2-TZVP are depicted in Figure 1. Two distinct conformations could be located. They are very close in energy with **1**-C2 being more stable at M06/def2-TZVP ( $\Delta H_{C1-C2}$  = +0.04 kcal/mol and

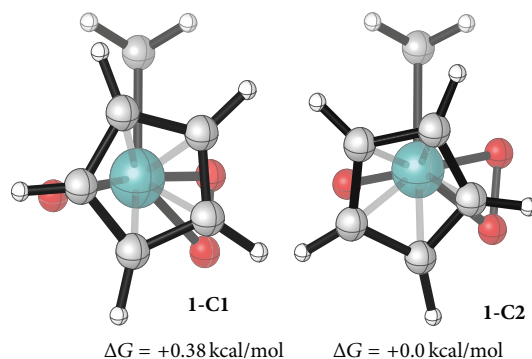


FIGURE 1: Illustrating the conformation differences.

TABLE 1: Key vibrational modes and their calculated frequencies.

	<b>1</b> -C1	<b>1</b> -C2
$\nu_{\text{Mo-O}}$	640.35, 625.81	635.75, 616.86
OOP C–H bending of Cp	849.88, 829.84, 818.68	847.10, 830.87, 821
$\nu_{\text{Mo=O}}$	1032.34	1028.21
In-plane C–H bending of Cp	1038.02	1039.12
$\nu_{\text{O-O}}$	1041.44	1040.97

$\Delta G_{C1-C2}$  = +0.38 kcal/mol). The effect of the Cp conformation on the vibrational frequencies is generally small (Table 1).

The normal modes of various key vibrational modes listed in Table 1 are depicted in Figures 2 and 3. In general, Mo–O, Mo=O, and O–O stretches are strongly coupled to vibration modes of the Cp ring (Figure 2) but the bending modes of Cp ring are not strongly coupled to the Mo( $\eta^2$ -O<sub>2</sub>)OCH<sub>3</sub> portion of **1**.

The normal modes associated with the bending of Cp ring are shown in Figure 3. The IP C–H bending was predicted to have a relative high intensity.

The various isotopes of Molybdenum have negligible effect on the frequencies. The difference is generally less than 10 cm<sup>-1</sup>; therefore, we would not be considering the effect of isotope in the calculations.

The effects of size of basis sets on the vibrational modes of interest and their frequencies are tabulated in Table 2. The O–O stretch is in all cases higher than the M=O stretch, except in the case of the smallest basis set, def2-SVP. However, the result at M06/def2-SVP is unlikely to be accurate, as the addition of diffuse function reversed the order (M06/def2-SVPD). Larger basis sets def2-TZVP and def2-TZVPD gave the same order as def2-SVPD.

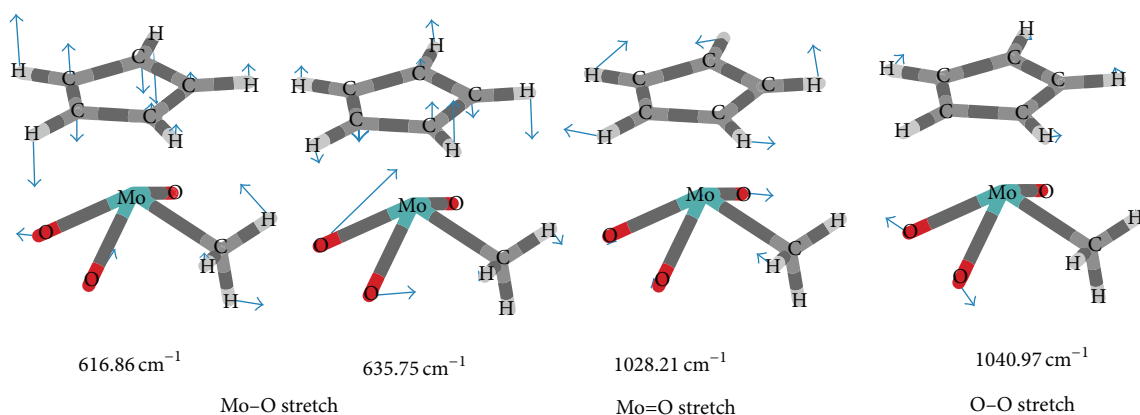
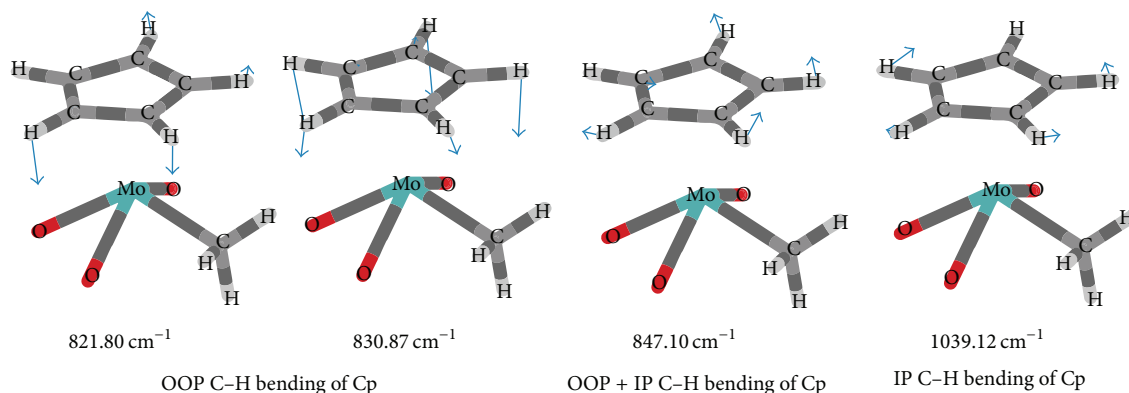
When the numerical accuracy is increased by employing a larger integration grid and tighter convergence criteria as implemented in Gaussian 09, the Mo=O stretch and O–O stretch become strongly coupled and assignment of frequency is ambiguous. However, at M06/def2-TZVP Mo=O stretch and O–O stretch remain decoupled.

Systematic error in calculated IR frequencies calculated by theoretical methods such as *ab initio* and DFT is well documented. Scaling factor has been determined for HF,

TABLE 2: Key vibration modes and their respective frequencies calculated at M06 with various basis sets.

Vibration mode	Expt. <sup>[a]</sup>	M06/def2-SVP	M06/def2-SVPD	M06/def2-TZVP	M06/def2-TZVPD
$\nu_{\text{Mo=O}}$	951	1042.41	1029.76	1028.21	1027.07
$\nu_{\text{O-O}}$	877	1036.81	1038.37	1040.97	1040.26
OOP bending C-H of Cp	N/A	813.94	821.31	830.87	826.03
$\nu_{\text{Mo-O}}$	565	637.30	626.28	635.75	634.37
		620.86	609.96	616.86	615.79

<sup>[a]</sup> Based on assignment based on the work of Al-Ajlouni et al. [30].

FIGURE 2: Normal modes associated with MoO( $\eta^2$ -O<sub>2</sub>) of 1-C2.FIGURE 3: 800–850 cm<sup>-1</sup> bending modes that are associated with the Cp ring for 1-C2.

MP2, and various DFT functionals with many different basis sets [32–35]. The order of frequencies is important as scaling could improve agreement with experimental frequencies, but it does not change the order of frequencies.

In order to ascertain that the reversed order of O–O stretch and Mo=O stretch frequencies when the M06 functional was used is not sensitive to the choice of basis set (other than the Weigend and Aldrich ones used), calculations were performed with the two variants of the LANL2 basis set for Molybdenum and the 6-311+G(d,p) or ACCT basis set for carbon, hydrogen, and oxygen atoms. As can be seen from Table 3, the order of  $\nu_{\text{O-O}}$  and  $\nu_{\text{Mo=O}}$  is not affected by the change of basis set.

Nevertheless, the problem could lie in the functional and could be largely independent of the basis set. Therefore, we

optimized the geometry of **1** with various DFT functionals and also MP2. The basis set is restricted to def2-TZVP for DFT and MP2 (def2-SVP and def2-SVP are included for comparison purpose as *ab initio* results are known to improve with increasing basis set size). The results are tabulated in Table 4. M06 is the outlier amongst all the methods employed in Table 4, as it predicts that  $\nu_{\text{O-O}}$  is higher in wavenumber than  $\nu_{\text{Mo=O}}$  in **1**.

It is likely that the assignment made by M06 is erroneous; therefore, it is not recommended for assignment of Molybdenum complexes which contain both Mo=O and O–O groups.

**3.1.1. Discrepancy between Calculated and XRD O–O Bond Length.** From Table 4, there is a large discrepancy between O–O bond lengths derived from XRD and calculations. It is

TABLE 3: Results at M06 with various basis sets as indicated in the table.

Mo	Basis set	Non-Mo	$\nu_{\text{Mo=O}}/\text{cm}^{-1}$	$\nu_{\text{O-O}}/\text{cm}^{-1}$	$\nu_{\text{Mo=O}} - \nu_{\text{O-O}}$	Mo=O/Å
LANL2TZ(f)	6-311 + G(d,p)		1000.02	1027.54	-27.52	1.669
	ACCT		1011.06	1040.92	-29.86	1.669
LANL2DZmod	6-311 + G(d,p)		987.63	1022.78	-35.15	1.695
	ACCT <sup>[a]</sup>		1010.59	1040.99	-30.4	1.684

<sup>[a]</sup> Invoked via the keyword “aug-cc-pVTZ” in Gaussian 09.

TABLE 4: Mo=O and O–O stretching, and Cp’s C–H OOP bending frequencies for **1**.

	$\nu_{\text{Mo=O}}/\text{cm}^{-1}$	$\nu_{\text{O-O}}/\text{cm}^{-1}$	$\nu_{\text{Mo=O}} - \nu_{\text{O-O}}/\text{cm}^{-1}$	$\nu_{\text{OOP bending C-H}}/\text{cm}^{-1}$	Mo=O/Å	O–O/Å
M06L	980.21	963.92	+16.29	828.80	1.685	1.430
M06	1028.21	1040.97	-12.76	830.87	1.670	1.408
M06-2X	1076.74	1060.31	+16.43	847.72	1.658	1.412
PBE0	1043.41	1031.92	+11.49	842.94	1.669	1.414
B3LYP	1017.40	977.41	+39.99	840.90	1.681	1.437
B3PW91	1030.09	1009.12	+20.97	839.89	1.675	1.422
MP2/def2-SVP	952.02	894.69	+57.33	816.75	1.708	1.457
MP2/def2-SVPD	936.88	871.31	+65.57	820.09	1.714	1.469
MP2/def2-TZVP	954.83	920.28	+34.55	826.25	1.711	1.459
Expt.	951 <sup>a</sup>	877 <sup>a</sup>	+74		1.728	1.271

<sup>a</sup> Based on assignment based on the work of Al-Ajlouni et al [30].

TABLE 5: Mo=O and O–O stretching, and Cp’s C–H OOP bending frequencies for **1-CF<sub>3</sub>**.

	$\nu_{\text{Mo=O}}/\text{cm}^{-1}$	$\nu_{\text{O-O}}/\text{cm}^{-1}$	$\nu_{\text{Mo=O}} - \nu_{\text{O-O}}/\text{cm}^{-1}$	Mo=O <sup>[a]</sup> /Å	O–O <sup>[a]</sup> /Å
M06L	976.99	967.87	9.12	1.685	1.427
M06	1028.87	1044.62	-15.75	1.669	1.404
M06-2X	1084.30	1065.57	18.73	1.656	1.409
Expt.	952.7 <sup>[b]</sup>			1.689	1.440

<sup>[a]</sup> Bond lengths are taken from the work of Hauser et al. [38]. <sup>[b]</sup> From the work of Hauser et al. [39], no assignment was made by them. We believe that Mo=O and O–O band may not be resolved, as the next strong band is at 891 cm<sup>-1</sup>.

TABLE 6: Mo=O and O–O stretching, and Cp’s C–H OOP bending frequencies for **1-Cl**.

	$\nu_{\text{Mo=O}}/\text{cm}^{-1}$	$\nu_{\text{O-O}}/\text{cm}^{-1}$	$\nu_{\text{Mo=O}} - \nu_{\text{O-O}}/\text{cm}^{-1}$	Mo=O/Å	O–O/Å
M06L	981.10	963.24	17.86	1.678	1.430
M06	1032.38	1040.76	-8.38	1.662	1.406
M06-2X	1085.37	1066.20	19.17	1.649	1.410
Expt.	881	842	39	1.771	1.352

Bond lengths and IR frequencies are taken from the work of Galakhov et al. [40].

unlikely that modern computational methods would give an error of such magnitude. Al-Ajlouni et al. have indicated that the crystal used for XRD is twinned and technical difficulties were encountered in solving the X-ray structure (supporting information of [30]).

Two other peroxo complexes were calculated: they are **1-CF<sub>3</sub>** and **1-Cl**. The XRD solution for **1-CF<sub>3</sub>** is of better quality than both **1** and **1-Cl**. This is indicated by multiple warning when the CIF files of **1** and **1-Cl** were subjected to checking by checkCIF [36]. Therefore, it would be more prudent to compare calculated bond lengths of **1-CF<sub>3</sub>** with those derived

from XRD. The results for this comparison are tabulated in Table 5.

From Table 5, the trend is similar to that of **1**. M06 functional predicted that O–O stretch would be of higher frequency than Mo=O stretch. The calculated O–O and Mo=O bond lengths are of much better agreement with XRD determined bond length.

Calculated frequencies for complex **1-Cl** gave the same trend as **1** and **1-CF<sub>3</sub>** (Table 6). Similar to **1**, checkCIF displayed several warnings for the CIF file of **1-Cl**. The discrepancy between XRD and calculated Mo=O and O–O

TABLE 7: Mo=O stretching and Cp's C-H OOP bending frequencies for **2**.

	$\nu_{\text{Mo=O, asym}}/\text{cm}^{-1}$	$\nu_{\text{Mo=O, sym}}/\text{cm}^{-1}$	$\nu_{\text{Mo=O, sym}} - \nu_{\text{Mo=O, asym}}/\text{cm}^{-1}$
M06L/def2-TZVP	946.29	973.92	27.63
M06/def2-TZVP	982.01	1013.78	31.77
M06-2X/def2-TZVP	1017.38 <sup>[a]</sup>	1059.88 <sup>[a]</sup>	42.5
PBE0/def2-TZVP	996.75	1027.54	30.79
B3LYP/def2-TZVP	975.30	1004.35	29.05
CAM-B3LYP/def2-TZVP	1006.55	1042.96	36.41
B3PW91/def2-TZVP	985.68	1015.36	29.68
wB97xD/def2-TZVP	1006.62	1044.62	38
MP2/def2-SVP	928.80	899.36	-28.64
MP2/def2-SVPD	903.11	884.42	-18.69
MP2/def2-TZVP	923.48	903.53	-19.95
Experimental <sup>[b]</sup>	918	887	-31

<sup>[a]</sup>Tight convergence criteria and ultrafine integration grid were used due to a low imaginary frequency when optimized with default setting. <sup>[b]</sup>Assignment based on the work of Legzdins et al.; see [29].

TABLE 8: Results of asymmetric and symmetric Mo=O stretches for  $\text{MoO}_4^{2-}$  at various levels of theory. See Figure 5.

Methods	$\nu_{\text{Mo=O, asym}}/\text{cm}^{-1}$	$\nu_{\text{Mo=O, sym}}/\text{cm}^{-1}$	$\nu_{\text{Mo=O, sym}} - \nu_{\text{Mo=O, asym}}$
MP2/def2-SVP	828.52	808.83	19.69
MP2/def2-SVPD	772.78	768.95	3.83
MP2/def2-TZVP	810.13	799.53	10.6
MP2/def2-TZVPD	786.31	789.21	-2.9
MP2/def2-QZVPD	783.53	789.82	-6.29
CCSD(T)/def2-SVP <sup>[a]</sup>	839.60, 840.17, 840.27	872.13	-32 (840-872)
M06L/def2-SVP	843.69	874.91	-31.22
M06L/def2-SVPD	818.43	860.74	-42.31
M06L/def2-TZVP	817.71	864.85	-47.14
M06L/def2-TZVPD	807.75	863.15	-55.4

<sup>[a]</sup>The optimized geometry does not have a  $T_d$  symmetry.

bond lengths is large, as in the case of **1**. We concluded that, in the case of **1** and **1-Cl**, the XRD derived O-O and Mo=O bond length is unlikely to be as reliable as the calculated one. This is similar to the conclusion made by Costa et al. [7].

**3.2. Vibrational Modes of  $\text{CpMoO}_2\text{CH}_3$ .** Geometries and vibrational frequencies of  $\text{CpMoO}_2\text{CH}_3$  **2** were initially calculated with the same set of methods as in Table 4. We would focus on the Mo=O stretching frequencies (Table 7). The higher wavenumber band is assigned to the asymmetric M=O stretch and the lower one to the symmetric stretch by Legzdins and coworkers [31]. However, calculations with various DFT functionals indicate that the assignment should be reversed. In this case, there is no discrepancy amongst all the DFT functionals employed. Interestingly and also rather disturbingly MP2 results are in stark contrast with DFT results. Therefore, two additional functionals, long range corrected CAM-B3LYP and wB97xD, were tested. However, the assignments remain unchanged.

In this case, we believe that MP2 does not give reliable assignment even with the def2-TZVP basis set. The reasons are discussed in the following paragraphs.

Firstly, the work of Butcher et al. on Molybdenum(VI) dihalide dioxide complexes assigned the lower  $905\text{ cm}^{-1}$  to the asymmetric Mo=O stretch and the higher  $940\text{ cm}^{-1}$  to the symmetric Mo=O stretch [37]. Consistent with the results of Butcher et al., calculation at M06L/def2-TZVP shows that the asymmetric M=O is at  $1003.50\text{ cm}^{-1}$  and the symmetric M=O stretch is at  $1042.63\text{ cm}^{-1}$ .

Secondly, when testing MP2 with def2-SVP, def2-SVPD, def2-TZVP, and def2-TZVPD on  $\text{MoO}_4^{2-}$ , we found that the symmetric Mo=O stretch (IR inactive) becomes higher in wavenumber than the asymmetric Mo=O stretches at def2-TZVPD (Table 8). When diffuse function is added, the difference between asymmetric and symmetric Mo=O stretches decreases for MP2 but increases for M06L. The accuracy of MP2 is dependent on the size of basis set; thus, the results at def2-QZVPD should be the most accurate; therefore, the asymmetric Mo=O stretch should be of lower wavenumber than the symmetric one. This indicates that for MP2 a very large basis set augmented with diffuse functions is required for accurate assignment of Mo=O stretches. However, this is computationally very expensive for most molecules that are relevant to Molybdenum catalysis.



TABLE 9: Results of asymmetric and symmetric Mo=O stretches for variuos Molybdenum and Tungsten complexes. See Figure 6.

Complex	Label	$\nu_{\text{Mo=O, sym}}$		$\nu_{\text{Mo=O, asym}}$	
		Expt.	Calc. <sup>[a]</sup>	Expt.	Calc. <sup>[a]</sup>
CpMo( $\eta^2$ -O <sub>2</sub> )OCH <sub>3</sub>	<b>1</b>	951 <sup>[b]</sup>	973.92	N/A	N/A
CpMo(O) <sub>2</sub> CH <sub>3</sub>	<b>2</b>	926 <sup>[b]</sup>	973.92	902 <sup>[b]</sup>	946.29
CpMo(O) <sub>2</sub> Cl	<b>3</b>	920 <sup>[d]</sup>	973.16	887 <sup>[d]</sup>	944.71
Cp*Mo( $\eta^2$ -O <sub>2</sub> )OCl	<b>4</b>	934 <sup>[e]</sup>	957.54 <sup>[i]</sup>	N/A	N/A
CpMo( $\eta^2$ -O <sub>2</sub> )OC≡C-Ph	<b>5</b>	953 <sup>[f]</sup>	974.82	N/A	N/A
Cp*W( $\eta^2$ -O <sub>2</sub> )OCH <sub>3</sub>	<b>6</b>	949 <sup>[b]</sup>	961.45	N/A	N/A
CpW(O) <sub>2</sub> CH <sub>3</sub>	<b>7</b>	943 <sup>[b]</sup>	981.20	899 <sup>[b]</sup>	941.29
Cp*W( $\eta^2$ -O <sub>2</sub> )OCH <sub>2</sub> Si(CH <sub>3</sub> ) <sub>3</sub>	<b>8</b>	941 <sup>[b]</sup>	958.74	N/A	N/A
<b>9</b>	<b>9</b>	963 <sup>[g]</sup>	979.34	N/A	N/A
MoO <sub>2</sub> Cl <sub>2</sub> (DMF) <sub>2+</sub>	<b>10</b>	940 <sup>[h]</sup>	987.68	905	957.31

<sup>[a]</sup> Calculated at M06L/def2-TZVP. <sup>[b]</sup> Al-Ajlouni et al.; see [30]. <sup>[c]</sup> Legzdins et al.; see [31]. <sup>[d]</sup> Cousin and Green; see [41]. <sup>[e]</sup> Trost and Bergman; see [42]. <sup>[f]</sup> Chandra et al.; see [43]. <sup>[g]</sup> Thiels and Eppinger; see [44]. <sup>[h]</sup> Butcher et al.; see [37]. <sup>[i]</sup> strongly coupled to O–O stretch.

TABLE 10: Results of O–O stretches for variuos Molybdenum and Tungsten complexes.

Complex <sup>[a]</sup>	Label	O–O		Scaled (cm <sup>-1</sup> ) by		
		Expt.	Calculated	Linear model <sup>[b]</sup>	0.9613	0.9595 <sup>[c]</sup>
CpMo( $\eta^2$ -O <sub>2</sub> )OCH <sub>3</sub>	<b>1</b>	877 <sup>[d]</sup>	963.92	926.12	926.62	925.27
Cp*Mo( $\eta^2$ -O <sub>2</sub> )OCl	<b>4</b>	884 <sup>[e]</sup>	953.84	914.14	916.93	915.59
CpMo( $\eta^2$ -O <sub>2</sub> )OC≡C-Ph	<b>5</b>	930–950 <sup>[f]</sup>	958.05	919.14	920.97	919.63
Cp*W( $\eta^2$ -O <sub>2</sub> )OCH <sub>3</sub>	<b>6</b>	860 <sup>[g]</sup>	926.13	881.20	890.29	888.99
Cp*W( $\eta^2$ -O <sub>2</sub> )OCH <sub>2</sub> Si(CH <sub>3</sub> ) <sub>3</sub>	<b>8</b>	868 <sup>[g]</sup>	923.74	878.36	887.99	886.70
<b>9</b>	<b>9</b>	870 <sup>[h]</sup>	940.32	898.07	903.93	902.61
			951.49	911.35	914.67	913.34

<sup>[a]</sup> Refer to Table 9 for molecular structure. <sup>[b]</sup> Linear equation is  $y = 1.1887x - 219.69$  with a  $R^2$  of 0.5801. <sup>[c]</sup> From the work of Kesharwani et al. for M06L/def2-TZVP [35]. <sup>[d]</sup> Al-Ajlouni et al.; see [30]. <sup>[e]</sup> Trost and Bergman; see [42]. <sup>[f]</sup> Chandra et al.; see [43]. <sup>[g]</sup> Legzdins et al.; see [31]. <sup>[h]</sup> Thiels and Eppinger; see [44].

The local DFT functional M06L offers reliable assignment in this case even with medium size basis set such as def2-SVP. The more accurate CCSD(T) was also tested with def2-SVP basis set. The results are similar to that obtained from M06L, thus lending credence to the validity of M06L.

**3.3. Scaling for Calculated Harmonic Frequency to Fundamental Frequency.** We then examined the Mo=O and O–O stretching frequencies in ten complexes containing Molybdenum or Tungsten by restricting the level of theory to M06L/def2-TZVP based on the results presented in the previous section on **1** and **2** and also because of the lower computational cost of a local DFT functional such as M06L [22]. The results are tabulated in Table 9 and Figure 6 for Mo=O stretch and Table 10 for O–O stretch.

We attempted to perform mode specific scaling for the Mo=O of complexes listed in Table 9 and Figure 6 by using linear regression to model the experimental fundamental frequencies as a function of the calculated harmonic frequencies. A linear model  $y = 1.1887x - 219.69$  with a  $R^2$  of 0.5801 was obtained ( $y$  is the experimental frequency and  $x$  is the calculated frequency at M06L/def2-TZVP). A scaling factor was also obtained by setting the intercept of the linear model to zero ( $y = 0.9613x$ ,  $R^2 = 0.5588$ ).

Attempt to perform linear regression on the data in Table 10 gave a very poor  $R^2$  of 0.1581 when a linear model ( $y = mx + c$ ) is used. A negative  $R^2$  is obtained when the intercept  $c$  is set to zero. Given the smaller dataset for O–O stretching and the poor correlation when attempting to fit the data to a linear model, we decided to exclude these data from fitting and instead used the linear model or scaling factor determined from Table 9 and Figure 6 to scale the calculated harmonic frequencies of Table 10.

Kesharwani et al. reported a scaling factor for fundamentals of 0.9595 at M06L/def2-TZVP [35]. The optimal scaling factor for Mo=O stretch fundamental determined from the set of data in Table 9 and Figure 6 is 0.9613 which is very close to that of Kesharwani et al. Alternatively, we have also determined a linear equation to fit the calculated harmonic frequencies to the observed fundamental frequencies (Table 11, footnote a). The unscaled RMSD for Mo=O stretch for results in Table 9 and Figure 6 is 40.4 cm<sup>-1</sup>, and scaling by all three methods improved the RMSD to about 15 cm<sup>-1</sup> (Table 11) which is smaller than the 26.65 cm<sup>-1</sup> reported by Kesharwani et al.

The agreement between experimental O–O stretching frequencies and calculated ones is not as good as those of Mo=O. The unscaled RMSD is larger at 80.72 cm<sup>-1</sup>.

TABLE 11: RMSD of predicted fundamental frequency of Mo=O and O–O stretch.

	Mo=O	O–O
RMSD ( $\text{cm}^{-1}$ ) at M06L/def2-TZVP	40.45	80.72
RMSD ( $\text{cm}^{-1}$ ) scaled with linear model <sup>[a]</sup>	15.05	41.75
RMSD ( $\text{cm}^{-1}$ ) scaled with a factor of 0.9613	15.43	44.66
RMSD ( $\text{cm}^{-1}$ ) scaled with a factor of 0.9595	15.49	43.38

<sup>[a]</sup> Linear equation is  $y = 1.1887x - 219.69$  with a  $R^2$  of 0.5801.

The RMSD is reduced by about 50% after scaling to about the same magnitude as the unscaled RMSD for Mo=O stretching and is larger than those reported by Kesharwani et al.

At this point, it would be prudent to discuss the validity of assigning IR bands that is in the range of 860–880  $\text{cm}^{-1}$ . From the work of Al-Ajlouni et al.,  $\text{CpMo}(\eta^2\text{-O}_2)\text{OCH}_3$  **1** shows strong IR bands at 575, 831, 849, and 931  $\text{cm}^{-1}$  beside those in Table 2 [30]. The authors have not attempted to assign these bands. Given the poor correlation when we attempt to fit the experimental O–O stretch in Table 10 and the large RMSD of calculated O–O after scaling (Table 11), reassignment of O–O stretch might be needed. Specifically, the scaled O–O stretch at M06L/def2-TZVP is about 922  $\text{cm}^{-1}$ ; therefore, the strong band at 931  $\text{cm}^{-1}$  could be a better candidate for the O–O stretch of **1**. It should be noted that our claim remains to be tested with further experiments (such isotopic substitution with  $^{17}\text{O}$ ).

Work of Postel et al. demonstrated through isotopic substitution with  $^{17}\text{O}$  that  $^{16}\text{O}$ – $^{16}\text{O}$  stretching of a Molybdenum complex is 898  $\text{cm}^{-1}$  while the Mo=O is 914  $\text{cm}^{-1}$  [45]. Although this is a different complex from **1**, it is interestingly and potentially helpful to know that the difference between Mo=O and O–O frequencies is 16  $\text{cm}^{-1}$ . This is much smaller than the 74  $\text{cm}^{-1}$  for **1** according to the assignment by Al-Ajlouni et al. [30] and is generally closer to the difference predicted by most of the DFT functionals in Table 4. Finally, we noted that Chandra et al. assign peak in the range of 930–950  $\text{cm}^{-1}$  to O–O stretch of peroxo in Mo complexes [43].

**3.4. Correlation between Calculated O–O Bond Length and O–O Stretching Frequencies.** Cramer and coworkers observed a fairly linear relationship between O–O stretching frequencies and O–O bond length in a diverse of molecules [46]. In our case, the linear correlation between calculated O–O stretching frequencies and O–O bond length is excellent ( $R^2$ , Figure 4).

**3.5. Solvent Effects on Calculated IR Frequencies.** With **1-CF<sub>3</sub>** as a model, we investigated the effect of solvents on the peroxo stretching and Mo=O stretch frequencies. Two solvents are investigated: they are water and acetonitrile. Although in practice, **1-CF<sub>3</sub>** might have limited solubility in these solvents, the effect of hydrogen bonding between water and oxygen

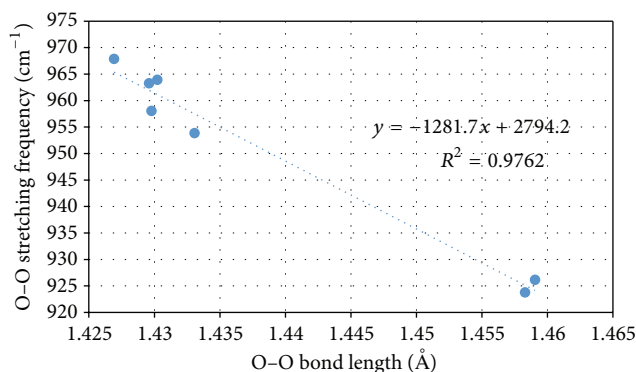


FIGURE 4: Plot of O–O stretching frequencies against O–O bond length for complexes reported in this work.

in **1-CF<sub>3</sub>** on O–O and M=O stretching frequencies could be interesting.

The results are tabulated in Table 12. Generally, both explicit and implicit solvation models predict a decrease in  $\nu_{\text{Mo=O}}$  and  $\nu_{\text{O–O}}$ . Given the limited data and lack of experimental data for validation, it is premature to draw further conclusion. The results presented in this section are intended to serve as preliminary guide to further study.

## 4. Conclusion

In this work, we have demonstrated the unsuitability of M06 functional for assignment of O–O and Mo=O frequency in **1**. We have also demonstrated that MP2 requires a large basis set with diffuse function to produce accurate order of asymmetric and symmetric Mo=O stretch. A series of complexes that calculated M06L/def2-TZVP indicates that symmetric M=O stretch (M=Mo or W) is generally higher in frequency than asymmetric M=O stretch. We found good agreement between experimental M=O stretches and calculated ones at M06L/def2-TZVP after scaling. However, peroxo stretching frequency remains problematic. As accurate assignment of IR bands to normal modes is crucial for kinetic study which employed in situ IR techniques, more work (both experimental and computational) on the assignment of peroxo stretching frequency in metal complexes is important.

## Abbreviations

- Cp: Cyclopentadienyl ligand  $\text{C}_5\text{H}_5$
- $\text{Cp}'$ : Cp and its derivative,  $\text{C}_5\text{R}_5$ , where R could be any groups such as  $\text{CH}_3$  in  $\text{Cp}^*$
- DFT: Density functional theory
- IR: Infrared
- IP: In plane
- OOP: Out of plane
- PCM: Polarizable continuum model
- RMSD: Root mean square deviation.

TABLE 12: Calculated Mo=O and O–O stretching frequencies in gas phase, with explicit solvation and with implicit solvation via PCM.

Level of theory	Solvent	$\nu_{\text{Mo=O}}/\text{cm}^{-1}$	$\nu_{\text{O-O}}/\text{cm}^{-1}$
M06L/def2-TZVP	No	976.99	967.87
	Acetonitrile, PCM <sup>[a]</sup>	944.48	959.34
	Acetonitrile, explicit <sup>[b]</sup>	952.75	961.73
	Water, PCM <sup>[a],[c]</sup>		960.28 <sup>[d]</sup>
	Water, explicit <sup>[b],[c]</sup>	959.20	968.15

<sup>[a]</sup> Default implicit solvent of Gaussian 09 A.02 was used. <sup>[b]</sup> Three molecules of solvents were added. <sup>[c]</sup> Tight convergence criteria and ultrafine integration grid were used due to low imaginary frequency with default setting. <sup>[d]</sup> Mo=O stretch and O–O stretch are strongly coupled, and assignment is ambiguous and therefore not attempted.

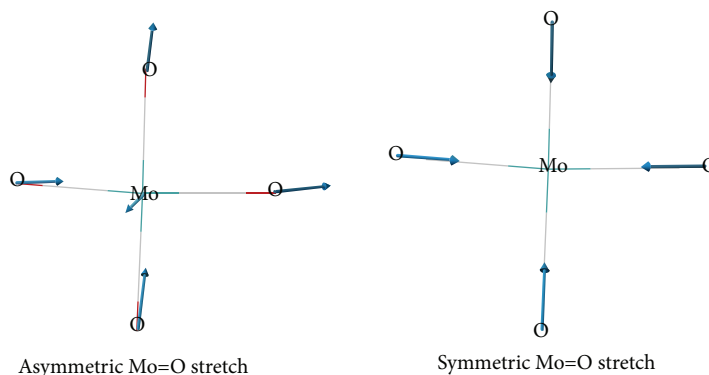


FIGURE 5

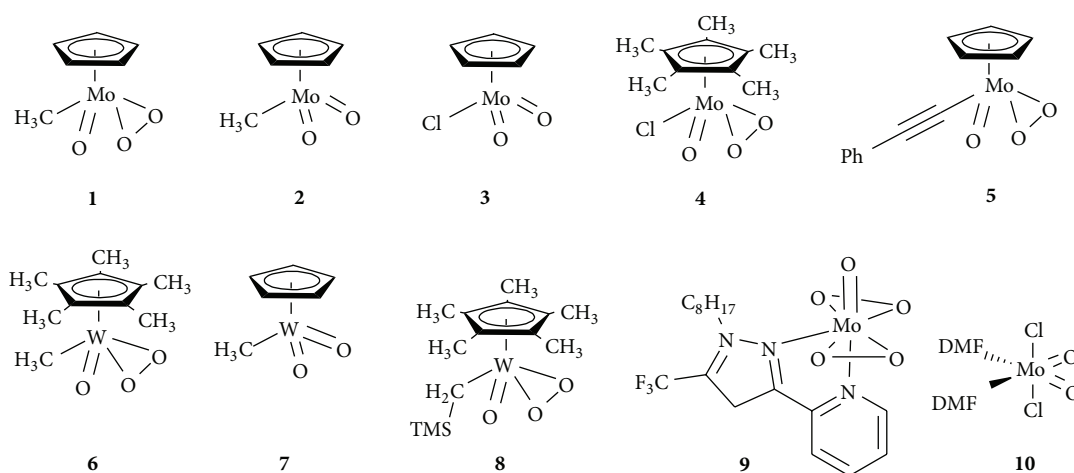


FIGURE 6

## Conflict of Interests

The author declares that there is no conflict of interests regarding the publication of this paper.

## Acknowledgments

Choon Wee Kee acknowledged C.-H Tan and NTU for funding and NUSHPC for generously providing free computational resources.

## References

- [1] F. E. Kühn, A. M. Santos, and M. Abrantes, "Mononuclear organomolybdenum(VI) dioxo complexes: synthesis, reactivity, and catalytic applications," *Chemical Reviews*, vol. 106, no. 6, pp. 2455–2475, 2006.
- [2] N. Grover and F. E. Kühn, "Catalytic olefin epoxidation with  $\eta^5$ -cyclopentadienyl molybdenum complexes," *Current Organic Chemistry*, vol. 16, no. 1, pp. 16–32, 2012.
- [3] S. A. Hauser, M. Cokoja, and F. E. Kühn, "Epoxidation of olefins with homogeneous catalysts—*quo vadis?*" *Catalysis Science & Technology*, vol. 3, no. 3, pp. 552–561, 2013.



- [4] Z. Wang, S. W. B. Ng, L. Jiang, W. J. Leong, J. Zhao, and T. S. A. Hor, "Cyclopentadienyl molybdenum(II) N,C-chelating benzothiazole-carbene complexes: synthesis, structure, and application in cyclooctene epoxidation catalysis," *Organometallics*, vol. 33, no. 10, pp. 2457–2466, 2014.
- [5] S. Li, C. W. Kee, K.-W. Huang, T. S. A. Hor, and J. Zhao, "Cyclopentadienyl molybdenum(II/VI) N-heterocyclic carbene complexes: synthesis, structure, and reactivity under oxidative conditions," *Organometallics*, vol. 29, no. 8, pp. 1924–1933, 2010.
- [6] Z. Wang, C. W. Kee, S. Li, T. S. A. Hor, and J. Zhao, "Aqueous phenol oxidation catalysed by molybdenum and tungsten carbonyl complexes," *Applied Catalysis A: General*, vol. 393, no. 1–2, pp. 269–274, 2011.
- [7] P. J. Costa, M. J. Calhorda, and F. E. Kühn, "Olefin epoxidation catalyzed by  $\eta^5$ -cyclopentadienyl molybdenum compounds: a computational study," *Organometallics*, vol. 29, no. 2, pp. 303–311, 2010.
- [8] M. Drees, S. A. Hauser, M. Cokoja, and F. E. Kühn, "DFT studies on the reaction pathway of the catalytic olefin epoxidation with CpMoCF<sub>3</sub> dioxo and oxo-peroxo complexes," *Journal of Organometallic Chemistry*, vol. 748, pp. 36–45, 2013.
- [9] A. Comas-Vives, A. Lledós, and R. Poli, "A computational study of the olefin epoxidation mechanism catalyzed by cyclopentadienyloxidomolybdenum(VI) complexes," *Chemistry: A European Journal*, vol. 16, no. 7, pp. 2147–2158, 2010.
- [10] S. F. Sousa, P. A. Fernandes, and M. J. Ramos, "General performance of density functionals," *The Journal of Physical Chemistry A*, vol. 111, no. 42, pp. 10439–10452, 2007.
- [11] Y. Zhao and D. G. Truhlar, "The M06 suite of density functionals for main group thermochemistry, thermochemical kinetics, noncovalent interactions, excited states, and transition elements: two new functionals and systematic testing of four M06-class functionals and 12 other functionals," *Theoretical Chemistry Accounts*, vol. 120, no. 1–3, pp. 215–241, 2008.
- [12] H. Kruse, L. Goerigk, and S. Grimme, "Why the standard B3LYP/6-31G\* model chemistry should not be used in DFT calculations of molecular thermochemistry: understanding and correcting the problem," *Journal of Organic Chemistry*, vol. 77, no. 23, pp. 10824–10834, 2012.
- [13] M. P. Waller, H. Kruse, C. Mück-Lichtenfeld, and S. Grimme, "Investigating inclusion complexes using quantum chemical methods," *Chemical Society Reviews*, vol. 41, no. 8, pp. 3119–3128, 2012.
- [14] P. Hobza, J. Šponer, and T. Reschel, "Density functional theory and molecular clusters," *Journal of Computational Chemistry*, vol. 16, no. 11, pp. 1315–1325, 1995.
- [15] L. F. Holroyd and T. van Mourik, "Insufficient description of dispersion in B3LYP and large basis set superposition errors in MP2 calculations can hide peptide conformers," *Chemical Physics Letters*, vol. 442, no. 1–3, pp. 42–46, 2007.
- [16] S. T. Schneebeli, A. D. Bochevarov, and R. A. Friesner, "Parameterization of a B3LYP specific correction for noncovalent interactions and basis set superposition error on a gigantic data set of CCSD(T) quality noncovalent interaction energies," *Journal of Chemical Theory and Computation*, vol. 7, no. 3, pp. 658–668, 2011.
- [17] Y. Zhao and D. G. Truhlar, "Applications and validations of the Minnesota density functionals," *Chemical Physics Letters*, vol. 502, no. 1–3, pp. 1–13, 2011.
- [18] M. J. Frisch, *Gaussian 09, Revision C.01*, Gaussian, Wallingford, Conn, USA, 2009.
- [19] F. Weigend and R. Ahlrichs, "Balanced basis sets of split valence, triple zeta valence and quadruple zeta valence quality for H to Rn: design and assessment of accuracy," *Physical Chemistry Chemical Physics*, vol. 7, no. 18, pp. 3297–3305, 2005.
- [20] D. Feller, "The role of databases in support of computational chemistry calculations," *Journal of Computational Chemistry*, vol. 17, no. 13, pp. 1571–1586, 1996.
- [21] K. L. Schuchardt, B. T. Didier, T. Elsethagen et al., "Basis set exchange: a community database for computational sciences," *Journal of Chemical Information and Modeling*, vol. 47, no. 3, pp. 1045–1052, 2007.
- [22] Y. Zhao and D. G. Truhlar, "A new local density functional for main-group thermochemistry, transition metal bonding, thermochemical kinetics, and noncovalent interactions," *The Journal of Chemical Physics*, vol. 125, no. 19, Article ID 194101, 2006.
- [23] C. Adamo and V. Barone, "Toward reliable density functional methods without adjustable parameters: the PBE0 model," *The Journal of Chemical Physics*, vol. 110, no. 13, pp. 6158–6170, 1999.
- [24] A. D. Becke, "Density-functional thermochemistry. III. The role of exact exchange," *The Journal of Chemical Physics*, vol. 98, no. 7, pp. 5648–5652, 1993.
- [25] T. Yanai, D. P. Tew, and N. C. Handy, "A new hybrid exchange-correlation functional using the Coulomb-attenuating method (CAM-B3LYP)," *Chemical Physics Letters*, vol. 393, no. 1–3, pp. 51–57, 2004.
- [26] J. P. Perdew, K. Burke, and Y. Wang, "Generalized gradient approximation for the exchange-correlation hole of a many-electron system," *Physical Review B*, vol. 54, no. 23, pp. 16533–16539, 1996.
- [27] J.-D. Chai and M. Head-Gordon, "Long-range corrected hybrid density functionals with damped atom-atom dispersion corrections," *Physical Chemistry Chemical Physics*, vol. 10, no. 44, pp. 6615–6620, 2008.
- [28] C. Y. Legault, *CYLVIEW*, Université de Sherbrooke, 2012.
- [29] P. Legzdins, E. C. Phillips, S. J. Rettig, L. Sánchez, J. Trotter, and V. C. Yee, "Remarkably inert metal-alkyl linkages in alkyl dioxo complexes of molybdenum and tungsten," *Organometallics*, vol. 7, no. 8, pp. 1877–1878, 1988.
- [30] A. M. Al-Ajlouni, D. Veljanovski, A. Capapé et al., "Kinetic studies on the oxidation of  $\eta^5$  cyclopentadienyl methyl tricarbonyl molybdenum(II) and the use of its oxidation products as olefin epoxidation catalysts," *Organometallics*, vol. 28, no. 2, pp. 639–645, 2009.
- [31] P. Legzdins, E. C. Phillips, and L. Sánchez, "New types of organometallic oxo complexes containing molybdenum and tungsten," *Organometallics*, vol. 8, no. 4, pp. 940–949, 1989.
- [32] M. W. Wong, "Vibrational frequency prediction using density functional theory," *Chemical Physics Letters*, vol. 256, no. 4–5, pp. 391–399, 1996.
- [33] I. M. Alecu, J. Zheng, Y. Zhao, and D. G. Truhlar, "Computational thermochemistry: scale factor databases and scale factors for vibrational frequencies obtained from electronic model chemistries," *Journal of Chemical Theory and Computation*, vol. 6, no. 9, pp. 2872–2887, 2010.
- [34] P. Sinha, S. E. Boesch, C. Gu, R. A. Wheeler, and A. K. Wilson, "Harmonic vibrational frequencies: scaling factors for HF, B3LYP, and MP2 methods in combination with correlation consistent basis sets," *The Journal of Physical Chemistry A*, vol. 108, no. 42, pp. 9213–9217, 2004.

- [35] M. K. Kesharwani, B. Brauer, and J. M. Martin, "Frequency and zero-point vibrational energy scale factors for double-hybrid density functionals (and other selected methods): can anharmonic force fields be avoided?" *The Journal of Physical Chemistry A*, vol. 119, no. 9, pp. 1701–1714, 2015.
- [36] checkCIF, 2015, <http://checkcif.iucr.org/>.
- [37] R. J. Butcher, H. P. Gunz, R. G. A. R. MacLagan, H. K. J. Powell, C. J. Wilkins, and Y. S. Hian, "Infrared spectra and configurations of some molybdenum(VI) dihalide dioxide complexes," *Journal of the Chemical Society, Dalton Transactions*, no. 12, pp. 1223–1227, 1975.
- [38] S. A. Hauser, R. M. Reich, J. Mink, A. Pöthig, M. Cokoja, and F. E. Kühn, "Influence of structural and electronic properties of organomolybdenum(II) complexes of the type  $[\text{CpMo}(\text{CO})_3\text{R}]$  and  $[\text{CpMo}(\text{O}_2)(\text{O})\text{R}]$  ( $\text{R} = \text{Cl}, \text{CH}_3, \text{CF}_3$ ) on the catalytic olefin epoxidation," *Catalysis Science & Technology*, vol. 5, no. 4, pp. 2282–2289, 2015.
- [39] S. A. Hauser, M. Cokoja, M. Drees, and F. E. Kühn, "Catalytic olefin epoxidation with a fluorinated organomolybdenum complex," *Journal of Molecular Catalysis A: Chemical*, vol. 363–364, pp. 237–244, 2012.
- [40] M. V. Galakhov, P. Gómez-Sal, T. Pedraz et al., "Cyclopentadienyl dithiocarbamate and dithiophosphate molybdenum and tungsten complexes," *Journal of Organometallic Chemistry*, vol. 579, no. 1–2, pp. 190–197, 1999.
- [41] M. Cousins and M. L. H. Green, "311. Some oxo- and oxochloro-cyclopentadienylmolybdenum complexes," *Journal of the Chemical Society (Resumed)*, pp. 1567–1572, 1964.
- [42] M. K. Trost and R. G. Bergman, " $\text{Cp}^*\text{MoO}_2\text{Cl}$ -catalyzed epoxidation of olefins by alkyl hydroperoxides," *Organometallics*, vol. 10, no. 4, pp. 1172–1178, 1991.
- [43] P. Chandra, S. L. Pandhare, S. B. Umbarkar, M. K. Dongare, and K. Vanka, "Mechanistic studies on the roles of the oxidant and hydrogen bonding in determining the selectivity in alkene oxidation in the presence of molybdenum catalysts," *Chemistry—A European Journal*, vol. 19, no. 6, pp. 2030–2040, 2013.
- [44] W. R. Thiel and J. Eppinger, "Molybdenum-catalyzed olefin epoxidation: ligand effects," *Chemistry: A European Journal*, vol. 3, no. 5, pp. 696–705, 1997.
- [45] M. Postel, C. Brevard, H. Arzoumanian, and J. G. Riess, "Oxygen-17 NMR as a tool for studying oxygenated transition-metal derivatives: first direct oxygen-17 NMR observations of transition-metal-bonded peroxidic oxygen atoms. Evidence for the absence of oxo-peroxo oxygen exchange in molybdenum(VI) compounds," *Journal of the American Chemical Society*, vol. 105, no. 15, pp. 4922–4926, 1983.
- [46] C. J. Cramer, W. B. Tolman, K. H. Theopold, and A. L. Rheingold, "Variable character of O–O and M–O bonding in side-on ( $\eta^2$ ) 1:1 metal complexes of  $\text{O}_2$ ," *Proceedings of the National Academy of Sciences of the United States of America*, vol. 100, no. 7, pp. 3635–3640, 2003.

